Case Report

Pathogenic Germ Line Variants in a Patient With Severe Toxicity From Breast Radiotherapy

Tyler J. Wilhite,[1] Ryan S. Youland,[1] Shulan Tian,[2] Randi R. Finley,[1] Jann N. Sarkaria,[1] Kimberly S. Corbin[1]

Clinical Practice Points

- While grade 3 or greater toxicity from adjuvant radiotherapy for breast cancer is uncommon, patients display a broad range of radiosensitivity.
- Uncommonly, breast cancer patients may develop severe toxicity from adjuvant radiotherapy, which may include extensive soft tissue fibrosis and cardiac dysfunction.
- DNA damage repair processes and maintenance of DNA integrity throughout replication are major contributors to radiosensitivity.
- A few rare genetic syndromes compromise DNA repair mechanisms, leading to enhanced radiosensitivity (eg, ataxia telangiectasia and Nijmegen breakage syndrome), but many patients with unexpectedly severe reactions to radiation will not have an identifiable syndrome.
- In the presence of severe radiation injury, whole-exome sequencing, when feasible, may provide plausible molecular explanations for enhanced toxicity.

Clinical Breast Cancer, Vol. 19, No. 3, e400-5
Keywords: Cardiac toxicity, DNA repair, DNA replication, Fibrosis, Genetic alterations, Radiosensitivity

Introduction

Adjuvant radiotherapy is indicated for many breast cancer patients after lumpectomy to reduce the risk of recurrence and improve overall survival.[1] Toxicity attributable to radiation is typically mild and may include fatigue, pruritus, and dermatitis acutely.[2,3] Regarding late toxicity, reported rates of moderate to severe fibrosis and telangiectasia are about 10%.[3-5] Although rare, severe acute and late radiation-related toxicities may occur in patients with an underlying genetic predisposition to extreme radiosensitivity[6,7] or in conditions associated with enhanced fibrotic reactions.[8]

We report the case of a woman treated with conventionally fractionated radiotherapy to the left breast and regional lymph nodes after lumpectomy who experienced unexpectedly severe toxicity and for whom germ line whole-exome sequencing (WES) was performed to identify potential genetic causes.

[1]Department of Radiation Oncology
[2]Division of Biomedical Statistics and Informatics, Department of Health Sciences Research, Mayo Clinic, Rochester, MN

Submitted: Dec 17, 2018; Revised: Feb 15, 2019; Accepted: Mar 12, 2019; Epub: Mar 28, 2019

Address for correspondence: Kimberly S. Corbin, MD, Department of Radiation Oncology, Mayo Clinic, 200 First Street SW, Rochester, MN 55905
E-mail contact: corbin.kimberly@mayo.edu

Case Report

A healthy 46-year-old woman sought care for a left breast mass in 1991. After mammography, excisional biopsy was performed, revealing grade 3 invasive ductal carcinoma that was positive for both estrogen receptor and progesterone receptor. Family history included a sister who died of breast cancer at age 51, a brother who died of leukemia at 64, and a sister who died of glioblastoma at 61. Her mother died of heart disease at 79, and her father, although diagnosed with lung cancer at 47, died of an unrelated cause at 74. She underwent genetic testing for germ line mutations in *TP53, BRCA1*, and *BRCA2*, which were negative. She had a 30 pack-year smoking history but quit in 1987.

She underwent lumpectomy with left axillary lymph node dissection. Negative margins were achieved. The primary tumor was pathologic T1b; 1 of 12 nodes was involved with adenocarcinoma. She then received 50.4 Gy in 28 fractions to the left breast and regional lymph nodes, followed by a boost of 14.4 Gy in 8 fractions to the lumpectomy bed (Figure 1). The estimated mean heart dose was 16.4 Gy, with a portion of the anterior heart receiving at least 30 Gy. After 10 fractions, she developed mild breast erythema that by the end of treatment worsened to moderate severity without desquamation. Radiotherapy was completed as planned without any interruptions due to adverse effects.

After radiotherapy, she received 6 cycles of cyclophosphamide, doxorubicin, and 5-fluorouracil, which were well tolerated. In

1526-8209/$ - see frontmatter
https://doi.org/10.1016/j.clbc.2019.03.004

Figure 1 Representative Images From Radiotherapy Treatment Plan Delivered in 1991, Reconstructed on Computed Tomography Scan From 1998

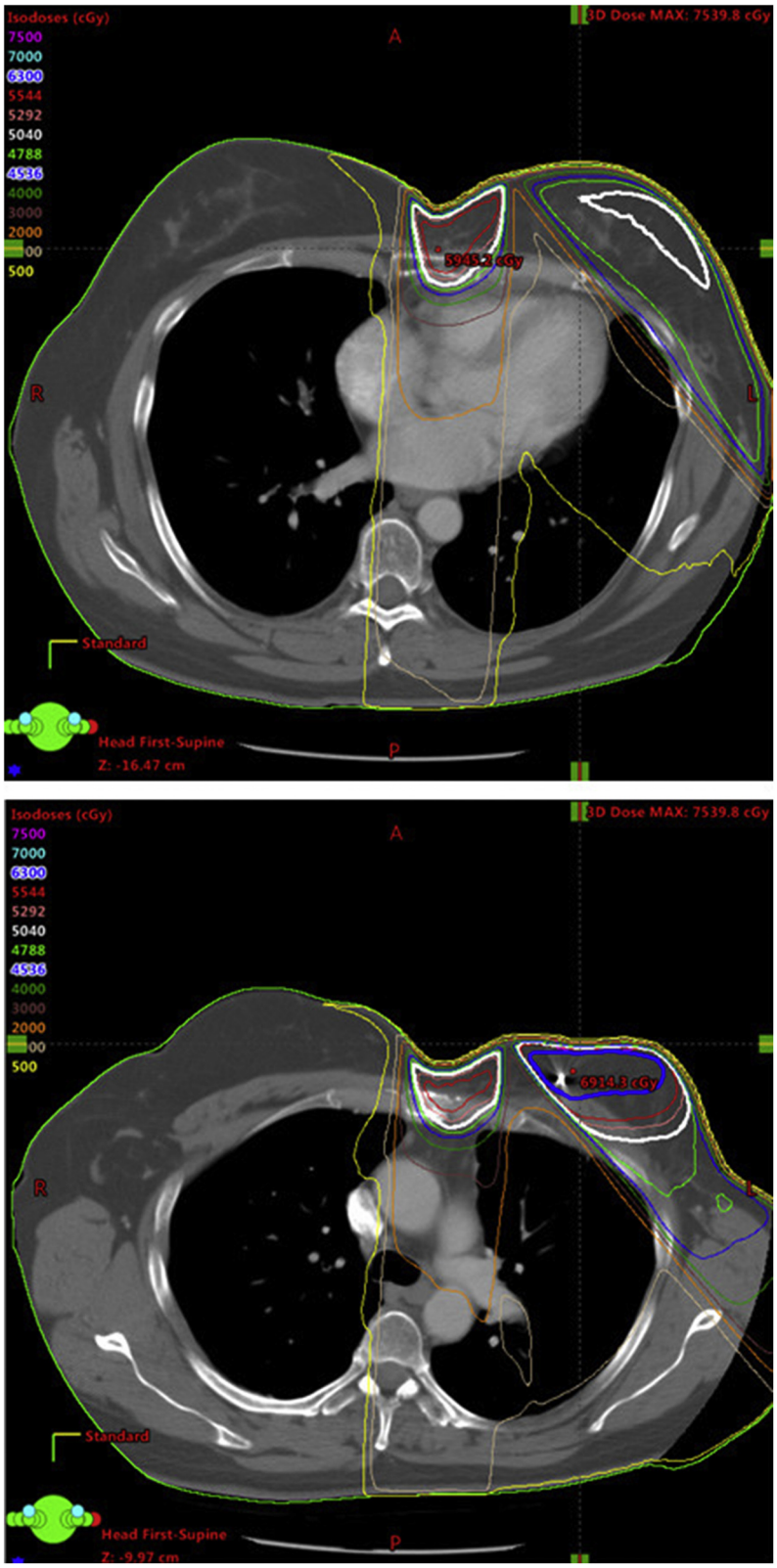

December 1992, she was admitted for chest pain. Cardiac assessment was negative. In January 1993, she again had chest pain. Echocardiogram revealed a 2.9 cm pericardial effusion with physiologic tamponade and a 15 mm Hg pulsus paradoxus. Pericardiocentesis drained 450 mL. Fluid cytology was bland, but the effusion reaccumulated the next day, when an additional 250 mL was drained. Symptoms resolved thereafter.

In the years that followed, she experienced intermittent chest pain, at times requiring opiates, as well as slowly worsening chest wall fibrosis. In 2007, an echocardiogram for syncope revealed mildly increased left ventricular filling pressure with an ejection fraction of 60%. A corresponding electrocardiogram showed evidence of sick sinus syndrome, which prompted pacemaker placement. That same year, computed tomography (CT) of the chest revealed extensive soft tissue and cardiac calcinosis (Figure 2). Endomyocardial biopsy was performed; results were negative for malignancy.

In June 2008, the chest wall fibrosis was more severe (Figure 3), and echocardiogram revealed severe right ventricular hypokinesis with preserved ejection fraction and no ischemia. Exertional dyspnea continued, and in May 2011, echocardiogram showed abnormal ventricular septal motion, new right ventricular enlargement, and reduced right ventricular systolic function. Pulmonary function testing showed reduced forced expiratory volume in 1 second (70% of predicted) and forced vital capacity (76% of predicted), attributed to restrictive physiology from chest wall fibrosis. In October 2012, an additional echocardiogram showed constrictive pericardial thickening with tethering of the right ventricle to the liver capsule. Ultimately her cardiologist initiated scheduled diuretic therapy, and subsequent echocardiograms demonstrated persistent but stable cardiac findings.

She was referred to our clinic in 2016 for recommendations on management of progressive late toxicity from radiation, with symptomatic calcinosis and chest wall pain. At that time, physical examination revealed severe chest wall fibrosis, telangiectasia, and marked breast retraction (Figure 3). We considered the possibility of a connective tissue disease, but antinuclear antibody and cyclic citrullinated peptide antibody tests were negative. In hopes of better understanding her severe toxicity, she consented to WES. After our visit, she initiated therapy with hyperbaric oxygen, pentoxifylline, and vitamin E, but as of her most recent follow-up in 2018, these therapies did not improve her pain or fibrosis.

Radiotherapy Plan Reconstruction

Radiotherapy to the left whole breast and regional lymph nodes was received at an outside institution in 1991. We obtained detailed records of this treatment, which included the linear accelerator parameters that were used. Additionally, we acquired a digital copy

Figure 2 Computed Tomography Scan From 2007 Showing Extensive Calcinosis Involving Sternum, Chest Wall, Pericardium, and Right Ventricle

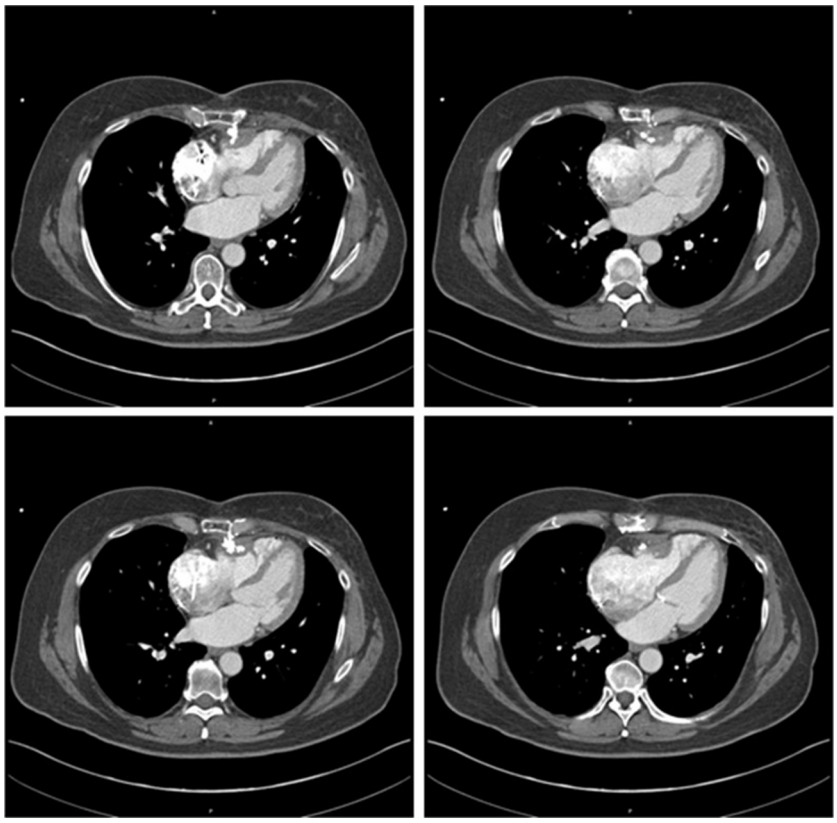

Figure 3 Extensive Radiation Fibrosis of Left Breast as It Appeared in 2008 (A) and 2016 (B), Along With Close-up View From 2014 (C)

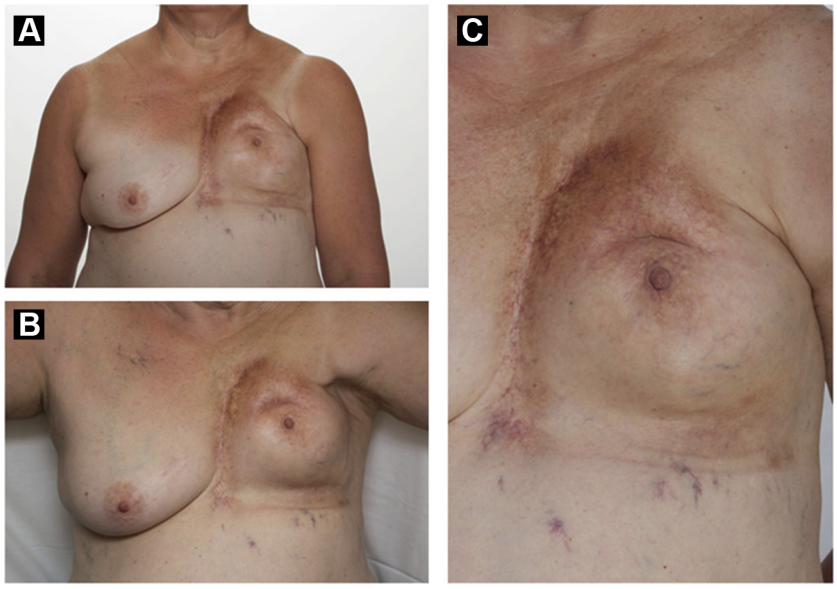

of CT imaging from 1998, as no earlier CT imaging was available, and uploaded it into Eclipse Treatment Planning System (Varian Medical Systems, Palo Alto, CA). After approximating isocenter on the CT data set, reported machine parameters were input into Eclipse for dose calculations to reconstruct her treatment plan. Representative slices are shown in Figure 1. The treatment technique consisted of 6 MV photon tangents with a half-beam block, matched to a 6 MV photon anteroposterior supraclavicular/internal mammary field. Internal mammary nodes were treated using 9 and 12 MeV electrons, while the lumpectomy bed was boosted with 9 MeV electrons.

Whole-Exome Sequencing

Peripheral blood was obtained as the source of genomic DNA. WES was performed in Mayo Clinic's medical genome facility. Paired-end sequencing libraries were prepared using 1.0 μg of genomic DNA. Whole-exome capture was carried out with the SureSelect Human All Exon V5+UTRs 75 MB kit (Agilent, Santa Clara, CA). The libraries were sequenced as 2 × 150 paired-end reads on the Illumina HiSeq 3000/4000 platform (Illumina, San Diego, CA). Base calling was performed using Illumina's RTA version 2.7.3. The average sequencing coverage across the exons was ~80×.

Analysis of Germ Line Alterations

Genome GPS is an internal comprehensive secondary analysis pipeline for WES data that integrates published variant calling methods. Secondary analysis entails 3 steps: alignment, single nucleotide and small insertion/deletion variant calling, and variation annotation. Unless otherwise specified, all tools were run under the default configuration. FASTQ files were/aligned to the hg19 reference genome using Novoalign version 3.02.04 with the following options: −hdrhd off −v 120 −c 4 −i PE 425,80 −x 5 −r Random (http://www.novocraft.com/). Realignment and recalibration were performed before the variations were detected with GATK's HaplotypeCaller version 3.3-0. Variant annotation was determined with Clinical Annotation of Variants (CAVA)[9] and Combined

Table 1 Genetic Variants Related to DNA Replication

Gene	CSN	Chr	Position	Ref	Alt	AD	SO	CAVA	CADD[a]	MAF
CDT1	c.535C > A_p.Pro179Thr	16	88871894	C	A	62, 48	Missense variant	Mod	19.8	$8.25E^{-6}$
MCM3	c.1393A > G_p.Thr465Ala	6	52141182	T	C	24, 25	Missense variant	Mod	27.2	$5.27E^{-4}$
PSMA6	c.78A > G_p.	14	35777201	A	G	25, 16	Splice region variant Synonymous variant	Mod	16.1	$1.13E^{-3}$

Abbreviations: AD = allelic depth (reference allele, alternative allele); Alt = alternative allele; CAVA = Clinical Annotation of Variants impact on protein (low, moderate [Mod], high); Chr = chromosome; CSN = clinical sequencing nomenclature; MAF = germ line minor allele frequency in ExAC consortium (> 60,000 whole-exome sequencing); SO = sequence ontology.
[a]CADD indicates Phred-like (−10 × log10(rank/total)) scaled C-score variant ranking relative to all possible substitutions of human genome (8.6E9). Scaled C-score ≥ 10 corresponds with 10% most deleterious variants in human genome. C-score ≥ 20 corresponds with 1% most deleterious.

Table 2 Genetic Variants Related to DNA Repair

Gene	CSN	Chr	Position	Ref	Alt	AD	SO	CAVA	CADD[a]	MAF
ATM	c.5071A > C_p.Ser1691Arg	11	108170506	A	C	33, 16	Missense variant	Mod	17.3	$2.02E^{-3}$
ATXN3	c.942_943insCAGCAGCAGCAGCAGCAGCAGCAG_p.Gln306_Gln314dup	14	92537354	C	—[b]	0, 61	In-frame insertion	Mod	10.5	0
DCLRE1A	c.2575A > T_p.Ile859Phe	10	115602192	T	A	141, 88	Missense variant	Mod	25.5	$2.67E^{-3}$
FANCI	c.1573A > G_p.Met525Val	15	89825056	A	G	86, 91	Missense variant	Mod	22.9	$2.13E^{-3}$
NBN	c.283G > A_p.Asp95Asn	8	90993640	C	T	23, 26	Missense variant	Mod	24.2	$1.86E^{-3}$
RECQL5	c.1586-5dupC	17	73626921	T	TG	14, 29	Intron variant Splice region variant	Low	6.3	0
SMC6	c.2677A > C_p	2	17876420	T	G	94, 102	Splice region variant Synonymous variant	Mod	16.0	$1.75E^{-3}$

Abbreviations: AD = allelic depth (reference allele, alternative allele); Alt = alternative allele; CAVA = CAVA impact on protein (low, moderate [Mod], high); Chr = chromosome; CSN = clinical sequencing nomenclature; Freq = germ line variant allele frequency based on ExAC consortium (> 60,000 whole-exome sequencing); MAF = germ line minor allele frequency in ExAC consortium (> 60,000 whole-exome sequencing); Ref = reference allele; SO = sequence ontology.
[a]CADD indicates Phred-like ($-10 \times \log10$(rank/total)) scaled C-score variant ranking relative to all possible substitutions of human genome (8.6E9). Scaled C-score ≥ 10 corresponds with 10% most deleterious variants in human genome. C-score ≥ 20 corresponds with 1% most deleterious.
[b]CCTGCTGCTGCTGCTGCTGCTGCTGCTG.

Annotation-Dependent Depletion (CADD).[10] Germ line variant allele frequency reported was based on the Exome Aggregation Consortium of over 60,000 genomes (ExAC, Broad Institute, Cambridge, MA)[11] and the 1000 Genomes Project.[12]

Genetic Alterations of Interest

From WES, 5209 total genetic variants were identified. After removing common variants (minor allele frequency > 1%), 608 functional variants remained. Of those, 34 were determined by CAVA to have high functional impact. Of those high-impact genes, none was determined to have an identifiable relationship to radiation toxicity or fibrosis. However, there were some genes, such as *C9orf131*, whose function was unknown and others, like *PABPC3*, with many functions but of unclear relation to radiosensitivity.[13] Hence, the contribution of these genetic alterations to severe toxicity in the patient is unclear.

Subsequent analyses focused on genes involved in DNA repair and replication because impairment of these processes is known to result in heightened sensitivity to radiation.[14,15] Specifically, there were alterations in 3 genes related to DNA replication and 7 genes related to DNA repair (Tables 1 and 2). Per CAVA, all but one of these variants were estimated to be of moderate functional impact. Compared with CAVA, CADD enables more detailed estimates of variant functional impact by generating C-scores that correlate with degree of pathogenicity.[10] Variants assigned C-scores of ≥ 10 rank among the most deleterious 10% of all possible variants in the human genome; scores of ≥ 20 rank among the most deleterious 1%.

In our patient, the variant estimated to be the most pathogenic was a missense mutation in *MCM3* (C-score = 27.2), resulting in a threonine-to-alanine substitution at position 465 on the corresponding MCM3 protein in a conserved domain near the arginine finger motif (positions 477 to 480).[16] MCM3 is one of 6 mini-chromosome maintenance proteins (MCM2-7) that form a heterohexamer with adenosine triphosphate (ATP)-driven helicase activity in the core of the DNA replication fork. These proteins are highly conserved from yeast to humans.[17] ATP hydrolysis, and hence helicase activity, is highly dependent on the alignment of the arginine finger motif in *MCM3* relative to the ATP binding site on *MCM7*.[18] As such, the variant observed near this region might impair DNA replication by reducing helicase activity at the replication fork.

The next most pathogenic variants involved DNA repair genes: single base pair substitutions in *DCLRE1A* (C-score = 25.5), *NBN* (C-score = 24.2), and *FANCI* (C-score = 22.9). *DCLRE1A* encodes for DNA cross-link repair 1A protein. There was an isoleucine-to-phenylalanine substitution at position 859, which in a known variant. In *DCLRE1A* yeast homolog, point mutations corresponding to positions 838 and 994 in the human protein each have been reported to result in increased sensitivity to DNA cross-links from cisplatin.[19] The observed mutation at position 859 may have resulted in similarly increased sensitivity to DNA cross-links, which are a potentially underappreciated aspect of DNA damage induced by ionizing radiation.[20]

FANCI mutations also have been observed to predispose to cross-link sensitivity,[21] and in FANCI protein, our patient showed a

methionine-to-valine mutation at position 525: two positions from the site of ubiquitination (lysine-523) required for DNA repair and cell cycle progression.[22] Nibrin protein (from NBN) is also integral to DNA repair, though in the recognition of double-strand breaks as a component of the MRN complex.[16] Our patient showed a point mutation at position 95 of nibrin, between the two domains essential for localization of the MRN complex and binding to histone H2AX: *FHA* (positions 24-83) and *BRCT* (positions 105-181).[23] Presumably, a mutation between these critical domains could alter their structure and function.

Conclusion

Our patient developed unexpectedly severe acute and late toxicity after radiotherapy for breast cancer. Though no sensitivities to radiotherapy were known before treatment, she experienced chronic pain, severe fibrosis with calcinosis, pericardial effusion from pericarditis, and cardiac dysfunction requiring a pacemaker. Modern radiotherapy planning, which in some cases entirely excludes the heart from the radiotherapy field, would be expected to reduce normal tissue exposure compared to her plan, but the degree of radiation-related change suggested enhanced sensitivity to radiotherapy.

WES identified several alterations ranked by CADD as among the top 1% most deleterious mutational possibilities in the human genome. Each of these variants is associated with a plausible mechanism for potentially increased radiation-related toxicity, specifically with regard to DNA replication fork helicase activity (*MCM3*), DNA cross-link repair (*DCLRE1A* and *NBN*), and double-strand break repair (*FANCI*). Further reports of germ line variants associated with severe toxicity to radiation are needed in order to guide the development of tools to predict radiosensitivity before radiotherapy administration. As germ line sequencing becomes more routine, institutions should consider maintaining registries of patients with idiosyncratic radiosensitivity to allow for systematic investigation.

Acknowledgments

This research was supported by the Mayo Clinic CCaTS grant UL1TR000135.

Disclosure

The authors have stated that they have no conflict of interest.

References

1. Darby S, McGale P, Correa C, et al. Effect of radiotherapy after breast-conserving surgery on 10-year recurrence and 15-year breast cancer death: meta-analysis of individual patient data for 10,801 women in 17 randomised trials. *Lancet* 2011; 378:1707-16.
2. Shaitelman SF, Schlembach PJ, Arzu I, et al. Acute and short-term toxic effects of conventionally fractionated vs hypofractionated whole-breast irradiation: a randomized clinical trial. *JAMA Oncol* 2015; 1:931-41.
3. Hamilton DG, Bale R, Jones C, et al. Impact of tumour bed boost integration on acute and late toxicity in patients with breast cancer: a systematic review. *Breast* 2016; 27:126-35.
4. De Santis MC, Bonfantini F, Di Salvo F, et al. Factors influencing acute and late toxicity in the era of adjuvant hypofractionated breast radiotherapy. *Breast* 2016; 29:90-5.
5. Whelan TJ, Pignol JP, Levine MN, et al. Long-term results of hypofractionated radiation therapy for breast cancer. *N Engl J Med* 2010; 362:513-20.
6. Gatti RA. The inherited basis of human radiosensitivity. *Acta Oncol* 2001; 40: 702-11.
7. Barnett GC, West CM, Dunning AM, et al. Normal tissue reactions to radiotherapy: towards tailoring treatment dose by genotype. *Nat Rev Cancer* 2009; 9: 134-42.
8. Gold DG, Miller RC, Petersen IA, Osborn TG. Radiotherapy for malignancy in patients with scleroderma: the Mayo Clinic experience. *Int J Radiat Oncol Biol Phys* 2007; 67:559-67.
9. Munz M, Ruark E, Renwick A, et al. CSN and CAVA: variant annotation tools for rapid, robust next-generation sequencing analysis in the clinical setting. *Genome Med* 2015; 7:15-195.
10. Kircher M, Witten DM, Jain P, O'Roak BJ, Cooper GM, Shendure J. A general framework for estimating the relative pathogenicity of human genetic variants. *Nat Genet* 2014; 46:310-5.
11. Karczewski KJ, Weisburd B, Thomas B, et al. The ExAC browser: displaying reference data information from over 60 000 exomes. *Nucleic Acids Res* 2017; 45: D840-5.
12. Auton A, Brooks LD, Durbin RM, et al. A global reference for human genetic variation. *Nature* 2015; 526:68-74.
13. O'Leary NA, Wright MW, Brister JR, et al. Reference sequence (RefSeq) database at NCBI: current status, taxonomic expansion, and functional annotation. *Nucleic Acids Res* 2016; 44:8.
14. Ward JF. DNA damage produced by ionizing radiation in mammalian cells: identities, mechanisms of formation, and reparability. *Prog Nucleic Acid Res Mol Biol* 1988; 35:95-125.
15. Borgmann K, Roper B, El-Awady R, et al. Indicators of late normal tissue response after radiotherapy for head and neck cancer: fibroblasts, lymphocytes, genetics, DNA repair, and chromosome aberrations. *Radiother Oncol* 2002; 64:141-52.
16. Consortium UniProt. UniProt: the universal protein knowledgebase. *Nucleic Acids Res* 2017; 45:D158-69.
17. Riera A, Barbon M, Noguchi Y, Reuter LM, Schneider S, Speck C. From structure to mechanism—understanding initiation of DNA replication. *Genes Dev* 2017; 31: 1073-88.
18. Davey MJ, Indiani C, O'Donnell M. Reconstitution of the Mcm2-7p heterohexamer, subunit arrangement, and ATP site architecture. *J Biol Chem* 2003; 278: 4491-9.
19. Ishiai M, Kimura M, Namikoshi K, et al. DNA cross-link repair protein SNM1A interacts with PIAS1 in nuclear focus formation. *Mol Cell Biol* 2004; 24:10733-41.
20. Dextraze ME, Gantchev T, Girouard S, Hunting D. DNA interstrand cross-links induced by ionizing radiation: an unsung lesion. *Mutat Res* 2010; 704:101-7.
21. Smogorzewska A, Matsuoka S, Vinciguerra P, et al. Identification of the FANCI protein, a monoubiquitinated FANCD2 paralog required for DNA repair. *Cell* 2007; 129:289-301.
22. Longerich S, San Filippo J, Liu D, Sung P. FANCI binds branched DNA and is monoubiquitinated by UBE2T-FANCL. *J Biol Chem* 2009; 284:23182-6.
23. Falck J, Coates J, Jackson SP. Conserved modes of recruitment of ATM, ATR and DNA-PKcs to sites of DNA damage. *Nature* 2005; 434:605-11.